The Coming Decades of Quantum Simulation

ICFO – Quantum Optics Theory

ICFO Institut de Ciències Fotòniques

PhD ICFO:

Bárbara Andrade **(many body, QI)**
Niccolò Baldelli **(many body, QI)**
Mohit Lal Bera **(QThermo)**
David Cirauqui Garcia **(MC optimization)**
Anna Dawid **(many body, ML, molecules)**
Jaime Díez Mérida **(exp)**
Gabriel Fernández Fernández **(ML, QI)**
Joana Fraxanet Morales **(many body)**
Katerina Gratsea **(ML)**
Nils-Eric Guenther **(many body)**
Sergi Julià Farré **(many body, Qthermo)**
Korbinian Kottmann **(QI, ML, many body)**
Guillem Müller Rigat **(many body)**
Jessica Oliveira de Almeida **(quantum optics, QI)**
Borja Requena Pozo **(ML)**
Tymoteusz Salamon **(many body)**

Postdocs ICFO:

Dr. Alexandre Dauphin **(many body, ML)**
Dr. Tobias Grass **(many body)**
Dr. Valentin Kasper **(many body, ML)**
Dr. Albert Aloy López **(QI)**
Dr. Luca Barbiero **(many body, QI)**
Dr. Utso Bhattacharya **(many body, atto)**
Dr. Irénée Frérot **(many body, QI)**
Dr. Daniel González Cuadra **(many body)**
Dr. Bernhard J. Irsigler **(many body)**
Dr. Andrew Maxwell **(atto)**
Dr. Gorka Muñoz Gil **(statistical phys, ML)**
Dr. Andrés Ordonñez **(atto)**
Dr. Reiko Yamada **(art&technoilogy)**

Ex-members and collaborators: Aditi Sen De, Ujjwal Sed (HRI, Alahabad), Manab Bera (IIT), François Dubin (CNRS), G. John Lapeyre (CSIC), Luca Tagliacozzo (UB), Alessio Celi (IQOQI/UAB), Matthieu Alloing (Paris), Tomek Sowiński (IFPAN), Phillip Hauke (Trento), Omjyoti Dutta (GMV), Christian Trefzger (EC), Kuba Zakrzewski (UJ, Cracow), Mariusz Gajda (IF PAN), Boris Malomed (Haifa), Ulrich Ebling (Kyoto), Bruno Julia Díaz (UB), Christine Muschik (UoT), Marek Kuś, Remigiusz Augusiak (CFT), Julia Stasińska (IFPAN), Alexander Streltsov (FUB), Ravindra Chhajlany (UAM), Fernando Cucchietti (MareNostrum), Anna Sanpera (UAB), Veronica Ahufinger (UAB), Tobias Grass (JQI,UMD/NIST), Jordi Tura (MPQ), Alexis Chacón (Los Alamos), Arnau Riera (BCN), Przemek Grzybowski (UAM), Swapan Rana (UW, Warsaw), Shi-Ju Ran (CNU), Irénée Frérot (ICFO-QIT), Giulia de Rosi (UPC), Maria Maffei (Grenoble), Christos Charampoulos (IFICS), Angelo Piga (WWW Institute)

Outline: Quantum Simulators of Lattice Gauge Theories

ICFO[R]
Institut
de Ciències
Fotòniques

1.1 Quantum Simulators: Ideology I

- **There exist many interesting quantum phenomena (such as superconductivity).**

- **These phenomena may have important applications!**

- **These phenomena are often difficult to be described and understood with the help of standard computers.**

- **Maybe we can use another, simpler and better controllable quantum system to simulate, understand and control these phenomena (R.P. Feynman)? Such a system would thus work as quantum computer of special purpose, i.e.**

QUANTUM SIMULATOR

Platforms:

Superconducting qubits

Ultracold atoms

Trapped ions

Rydberg atoms

Circuit QED

Photonics systems ...

Tasks/Goals

Classical/quantum optimization problems for technology

Quantum chemistry

Fundamental problems of physics

Systems:

"Paradigmatic", notoriously difficult, but relevant systems

Fundamental systems of condensed matter, HEP and QFT

Novel Quantum sImulAtors (NOQIA)

Novel systems, novel physics

Diagnostics/Design

Single cite/single "particle" resolution

Entanglement/topology characterization (random unitaries)

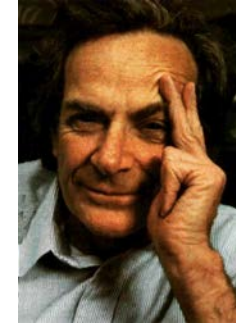Entanglement characterization (experiment-friendly approaches)

Topology characterization (experiment-friendly approaches)

Synthetic dimensions

Systems:

"Paradigmatic", notoriously difficult, but relevant systems

Fundamental systems of condensed matter, HEP and QFT

Novel Quantum sImulAtors (NOQIA)

Novel systems, novel physics

RESEARCH

QUANTUM SIMULATIO

String patt
Hubbard m

Christie S. Chiu[1], Geoffr
Eugene Demler[1], Fabian

Understanding strongly
most difficult challenge:
open questions on the p
strongly correlated elec
Hamiltonian and search
many realizations of str
Upon doping a cold-ato
strings, entities that ma
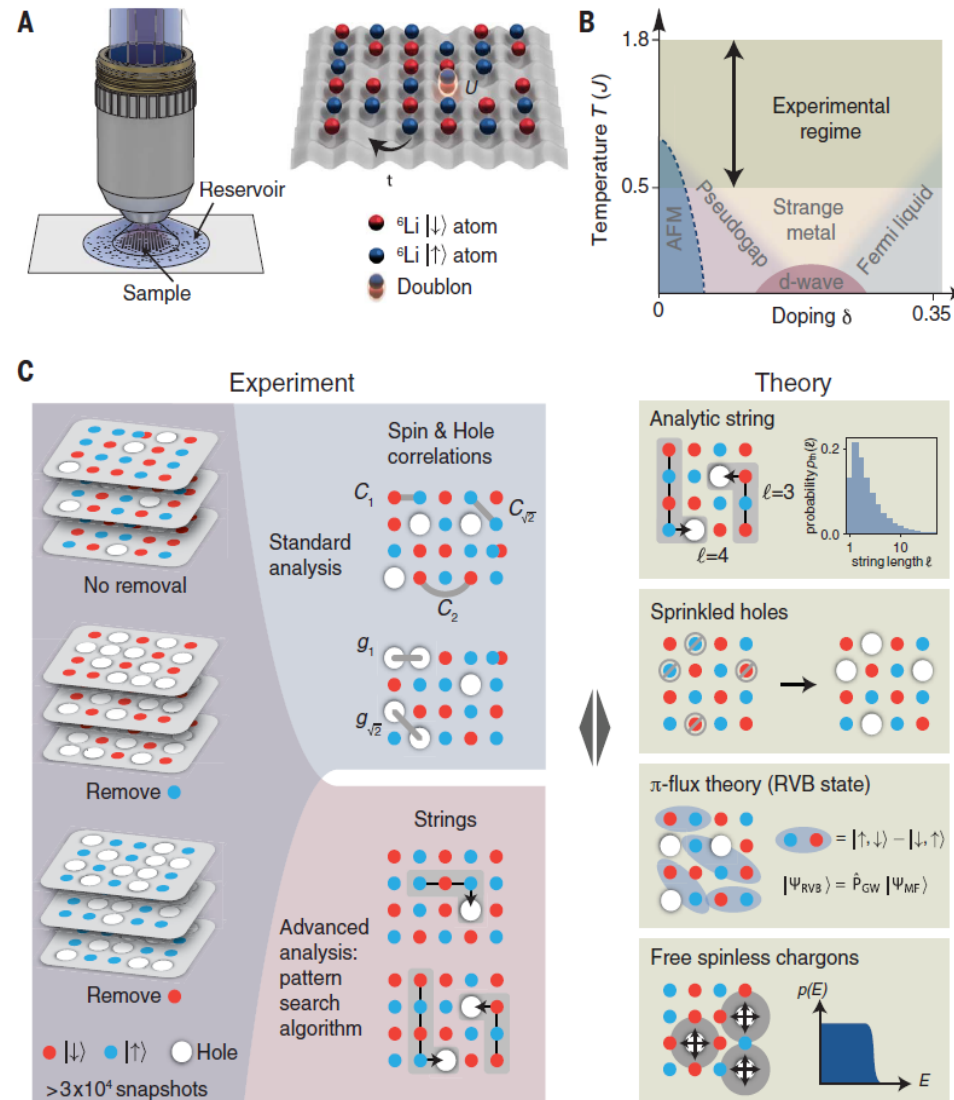order, in both pattern-b
the potential for patter
many-body systems.

theories for the doped
model

e Fermi-Hubbard model, which is
he Hamiltonian

$$-t \sum_{\sigma=\uparrow,\downarrow} \sum_{\langle \mathbf{ij} \rangle} (\hat{c}^\dagger_{\mathbf{i},\sigma} \hat{c}_{\mathbf{j},\sigma} + \text{h.c.})$$
$$+ U \sum_{\mathbf{j}} \hat{c}^\dagger_{\mathbf{j},\uparrow} \hat{c}_{\mathbf{j},\uparrow} \hat{c}^\dagger_{\mathbf{j},\downarrow} \hat{c}_{\mathbf{j},\downarrow} \qquad (1)$$

. The first term describes tunneling
e t of spin-½ fermions $\hat{c}_{\mathbf{j},\sigma}$ with spin
adjacent sites $\mathbf{i}$ and $\mathbf{j}$ of a two-
l square lattice. The second term
-site interactions of strength U be-
ons of opposite spin. We consider
correlated regime, where $U \gg t$ and
pied sites are energetically costly.
-Hubbard model is well understood
nd is half-filled at an average of one
site (Fig. 1B). For temperatures $T \ll J$,
t^2/U is the superexchange coupling,
tions appear. Although these mag-
ations are finite-ranged at nonzero
s, sufficiently cold finite-size systems
M order across the entire system (11).

Fig. 1. Quantum simulation of the Hubbard model. (**A**) Quantum gases trapped in optical lattices realize the Hubbard model with tunable on-site interaction U and nearest-neighbor hopping t. Quantum gas microscopy enables site-resolved readout of the quantum state. (**B**) Schematic of the conjectured phase diagram of the finite-size 2D Hubbard model with the experimentally accessed regime (green shading). (**C**) Outline of experimental observables used and theoretical models evaluated. We evaluate theories using both standard observables and pattern-recognition–based observables using snapshots of the quantum state.

Systems:

"Paradigmatic", notoriously difficult, but relevant systems

Fundamental systems of condensed matter, HEP and QFT

Novel Quantum sImulAtors (NOQIA)

Novel systems, novel physics

ARTICLE

There are amendments to this paper

Self-verifying variational quantum simulation of lattice models

C. Kokail[1,2,3], C. Maier[1,2,3], R. van Bijnen[1,2,3], T. Brydges[1,2], M. K. Joshi[1,2], P. Jurcevic[1,2], C. A. Muschik[1,2], P. Silvi[1,2], R. Blatt[1,2], C. F. Roos[1,2] & P. Zoller[1,2]*

Hybrid classical–quantum algorithms aim to variationally solve optimization problems using a feedback loop between a classical computer and a quantum co-processor, while benefiting from quantum resources. Here we present experiments that demonstrate self-verifying, hybrid, variational quantum simulation of lattice models in condensed matter and high-energy physics. In contrast to analogue quantum simulation, this approach forgoes the requirement of realizing the targeted Hamiltonian directly in the laboratory, thus enabling the study of a wide variety of previously intractable target models. We focus on the lattice Schwinger model, a gauge theory of one-dimensional quantum electrodynamics. Our quantum co-processor is a programmable, trapped-ion analogue quantum simulator with up to 20 qubits, capable of generating families of entangled trial states respecting the symmetries of the target Hamiltonian. We determine ground states, energy gaps and additionally, by measuring variances of the Schwinger Hamiltonian, we provide algorithmic errors for the energies, thus taking a step towards verifying quantum simulation.

ARTICLI

Self-verify

simulation

C. Kokail[1,2,3], C. Maier[1,2,3], R. van ...uschik[1,2], P. Silvi[1,2], R. Blatt[1,2],
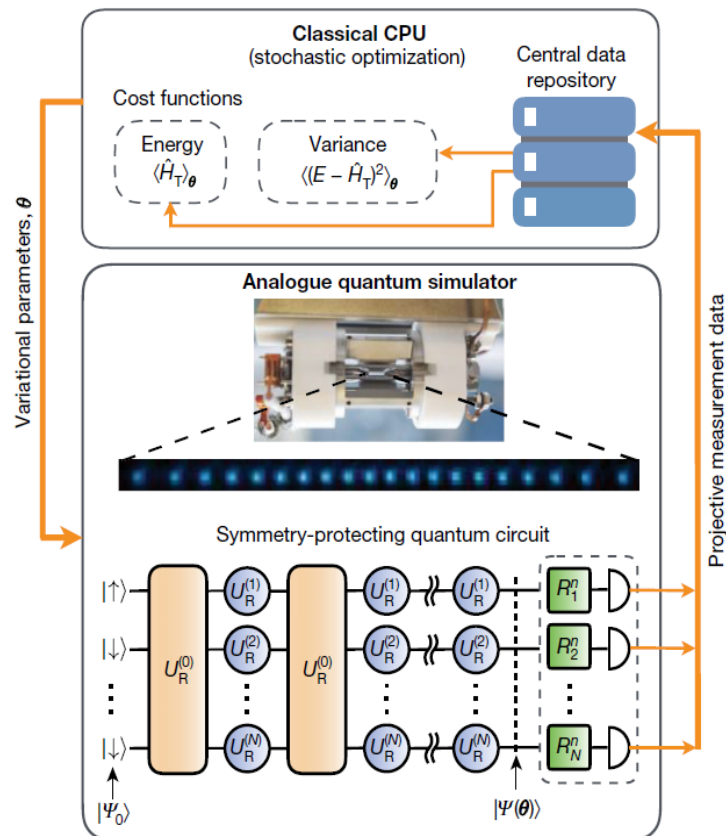C. F. Roos[1,2] & P. Zoller[1,2]*

ntum

Fig. 1 | Classical–quantum feedback loop of VQS. Optimization of cost functions with function evaluations performed on a programmable 20-qubit (blue dots) trapped-ion analogue quantum simulator. Variational control parameters are passed to the analogue quantum simulator, which generates trial states $|\Psi(\theta)\rangle$ through quench dynamics from a set of resource Hamiltonians with symmetry-protecting quantum circuits, consisting of entangling operations (orange boxes) and single-qubit operations (shaded blue circles), corresponding to quantum resources. Measurement results for correlation functions are obtained by rotating the qubits to the proper basis (green boxes) followed by quantum projective measurements in the standard basis. A central data repository stores the information on the obtained many-body correlation functions and allows for data re-evaluation for different Hamiltonian parameters (see Methods). The classical central processing unit (CPU) optimizes the parameters θ based on the measurement outcomes.

Hybrid classical–quantum alg...
classical computer and a quant...
that demonstrate self-verifyi...
high-energy physics. In cont...
the targeted Hamiltonian dire...
target models. We focus on the...
Our quantum co-processor is ...
generating families of entangl...
states, energy gaps and addit...
errors for the energies, thus t...

...using a feedback loop between a
...es. Here we present experiments
...odels in condensed matter and
...oes the requirement of realizing
...variety of previously intractable
...ional quantum electrodynamics.
...r with up to 20 qubits, capable of
...miltonian. We determine ground
...ltonian, we provide algorithmic

Confinement and Lack of Thermalization after Quenches in the Bosonic Schwinger Model

Titas Chanda[1,*] Jakub Zakrzewski[1,2] Maciej Lewenstein[3,4] and Luca Tagliacozzo[5,6]

[1]*Instytut Fizyki Teoretycznej, Uniwersytet Jagielloński, Łojasiewicza 11, 30-348 Kraków, Poland*
[2]*Mark Kac Complex Systems Research Center, Jagiellonian University in Krakow, Łojasiewicza 11, 30-348 Kraków, Poland*
[3]*ICFO-Institut de Ciències Fotòniques, The Barcelona Institute of Science and Technology,*
Av. Carl Friedrich Gauss 3, 08860 Castelldefels (Barcelona), Spain
[4]*ICREA, Passeig Lluis Companys 23, 08010 Barcelona, Spain*
[5]*Department of Physics and SUPA, University of Strathclyde, Glasgow G4 0NG, United Kingdom*
[6]*Depart ment de Física Quàntica i Astrofísica and Institut de Ciències del Cosmos (ICCUB), Universitat de Barcelona,*
Martí i Franquès 1, 08028 Barcelona, Catalonia, Spain

We excite the vacuum of a relativistic theory of bosons coupled to a $U(1)$ gauge field in $1 + 1$ dimensions (bosonic Schwinger model) out of equilibrium by creating a spatially separated particle-antiparticle pair connected by a string of electric field. During the evolution, we observe a strong confinement of bosons witnessed by the bending of their light cone, reminiscent of what has been observed for the Ising model [Nat. Phys. **13**, 246 (2017)]. As a consequence, for the timescales we are able to simulate, the system evades thermalization and generates exotic asymptotic states. These states are made of two disjoint regions, an external deconfined region that seems to thermalize, and an inner core that reveals an area-law saturation of the entanglement entropy.
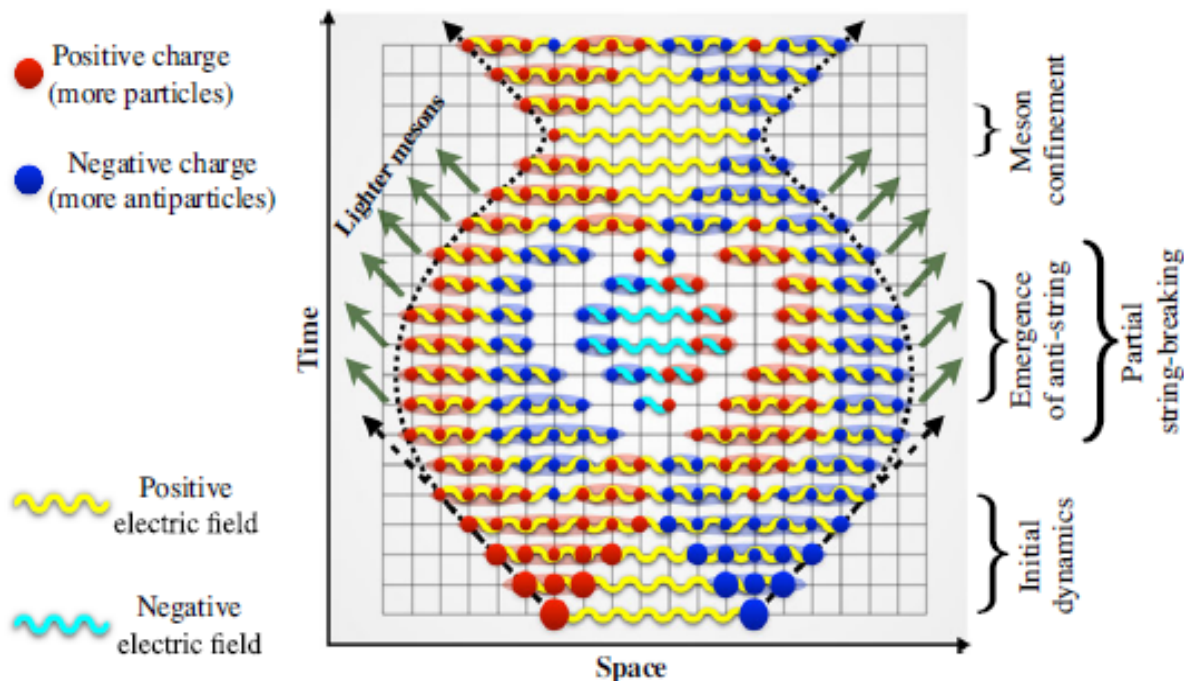
FIG. 1. Semiclassical sketch of the confining dynamics of BSM. We prepare a well-separated pair of particle and anti-particle connected by an electric-flux tube. Initially they start spreading as if they were free, however, their trajectories bend due to the energetic cost of creating larger electric-flux tubes. New dynamical charges are also created during the evolution and partially screen the electric field. Still the electric field oscillates coherently and can form an antistring, creating a central core of strongly correlated bosons. The density of bosons in the core can get depleted through the radiation of lighter mesons that freely propagate.

Systems:

"Paradigmatic", notoriously difficult, but relevant systems

Fundamental systems of condensed matter, HEP and QFT

Novel Quantum sImulAtors (NOQIA)

Novel systems, novel physics
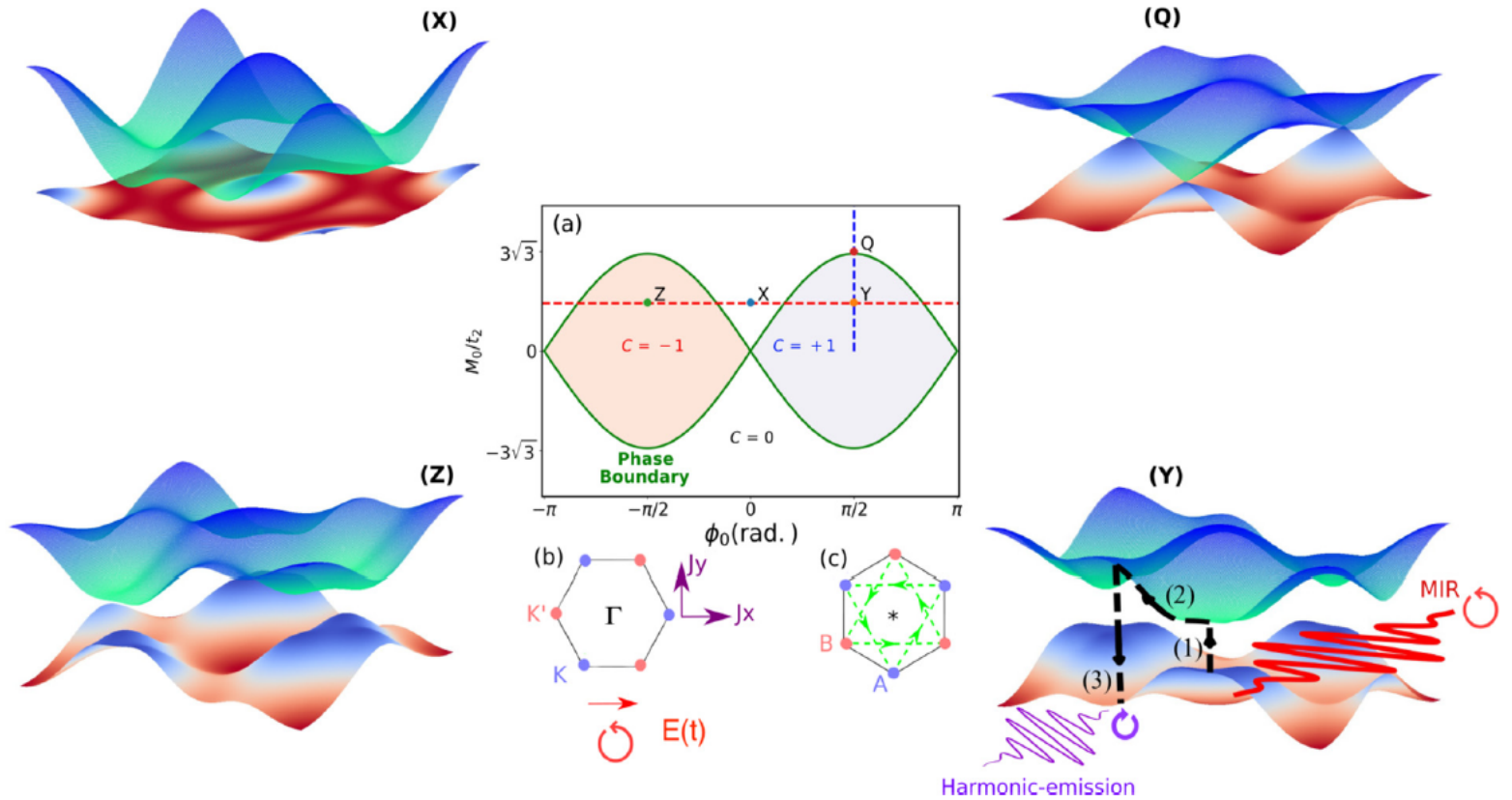
FIG. 1. Phase diagram and band structures of the Haldane model. (a) Phase diagram in the plane (ϕ_0, M_0/t_2), with the different phases labeled by their Chern number C; the green line shows the boundary of the topological phase transition. The band-structure diagrams correspond to the points X, Y, Z, and Q as marked in (a), with the point Q at the phase transition showing the gapless Dirac cone at the K point. (Y) and (Z) depict the band structure when the conduction-band topological invariants are $C = \pm 1$ at the phase points $\phi_0 = \pm\pi/2$ and $M_0 = 2.54t_2$. (Y) shows how the midinfrared laser-source oscillations (red-solid line) drive the topological material; this can be with both linear and circular polarizations. We also depict a physical cartoon of the electron-hole pair dynamics driven by a linearly polarized laser, i.e., creation, propagation, and annihilation or recombination by the black-dashed lines with arrows, and finally the subsequent harmonic emission (violet oscillations). The dashed lines in (a) indicate the cuts used for the parameter scans below. Panels (b) and (c) show the Brillouin zone and the real-space lattice of the Haldane model with the couplings in use.

Systems:

"Paradigmatic", notoriously difficult, but relevant systems

Fundamental systems of condensed matter, HEP and QFT

Novel Quantum sImulAtors (NOQIA)

Novel systems, novel physics

Robust Topological Order in Fermionic $\mathbb{Z}_2$ Gauge Theories: From Aharonov-Bohm Instability to Soliton-Induced Deconfinement

Daniel González-Cuadra [1,*] Luca Tagliacozzo,[2] Maciej Lewenstein,[1,3] and Alejandro Bermudez[4]

[1]*ICFO—Institut de Ciències Fotòniques, The Barcelona Institute of Science and Technology, Avinguda Carl Friedrich Gauss 3, 08860 Castelldefels (Barcelona), Spain*
[2]*Departament de Física Quàntica i Astrofísica and Institut de Ciències del Cosmos (ICCUB), Universitat de Barcelona, Martí i Franquès 1, 08028 Barcelona, Spain*
[3]*ICREA, Lluis Companys 23, 08010 Barcelona, Spain*
[4]*Departamento de Física Teórica, Universidad Complutense, 28040 Madrid, Spain*

Topologically ordered phases of matter, although stable against local perturbations, are usually restricted to relatively small regions in phase diagrams. Thus, their preparation requires a precise fine-tunning of the system's parameters, a very challenging task in most experimental setups. In this work, we investigate a model of spinless fermions interacting with dynamical $\mathbb{Z}_2$ gauge fields on a cross-linked ladder and show evidence of topological order throughout the full parameter space. In particular, we show how a magnetic flux is spontaneously generated through the ladder due to an Aharonov-Bohm instability, giving rise to topological order even in the absence of a plaquette term. Moreover, the latter coexists here with a symmetry-protected topological phase in the matter sector, which displays fractionalized gauge-matter edge states and intertwines with it by a flux-threading phenomenon. Finally, we unveil the robustness of these features through a gauge frustration mechanism, akin to geometric frustration in spin liquids, allowing topological order to survive to arbitrarily large quantum fluctuations. In particular, we show how, at finite chemical potential, topological solitons are created in the gauge field configuration, which bound to fermions and form $\mathbb{Z}_2$ deconfined quasiparticles. The simplicity of the model makes it an ideal candidate for 2D gauge theory phenomena, as well as exotic topological effects, to be investigated using cold-atom quantum simulators.

Robust Topologi...   ... Aharonov-Bohm

Daniel González...   ...ejandro Bermudez[4]

^{1}ICFO—Ins...   ...l Technology,

A...   ...pain

^{2}Departame...   ...nos (ICCUB),

...   ...in

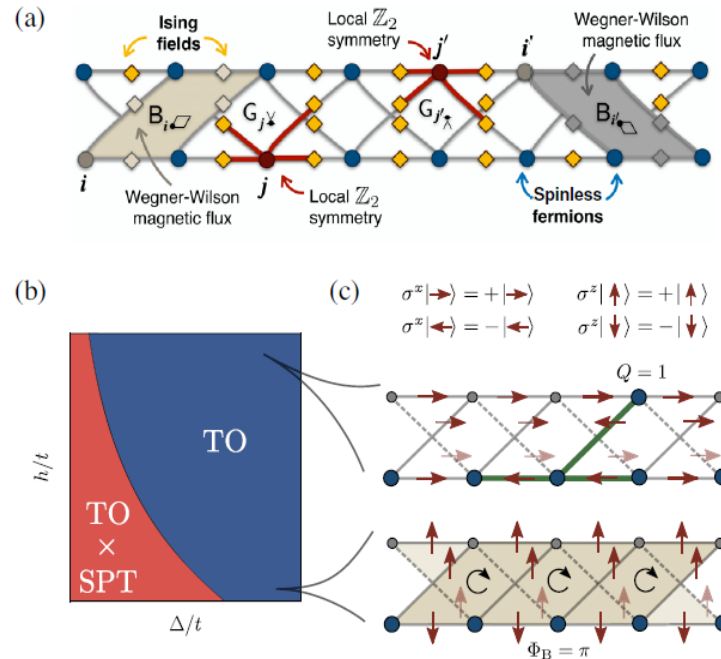^{4}Depa...   ...d, Spain

FIG. 1.   Creutz-Ising ladder. (a) Spinless fermions, which reside on the sites of a two-leg ladder (filled circles) and can tunnel along and across the legs forming a cross-linked pattern. These tunnelings are minimally dressed by Ising spin-$1/2$ fields, which sit on the corresponding links (filled rhombi). We represent the Wegner-Wilson fluxes across the two minimal plaquettes (tilted trapezes in grey) and the generators of the local $\mathbb{Z}_2$ symmetries (red graphs). (b) Sketch of the phase diagram at half filling in terms of the electric field h and the imbalance Δ. We find two phases, both with topological order (TO). In one case, the latter coexists with a SPT in the matter sector. (c) For $\Delta \gg t$, the fermions populate the lower leg of the ladder. At $h \ll t$, the Ising fields rearrange to spontaneously generate a π flux per plaquette through an Aharonov-Bohm instability, giving rise to TO. For $h \gg t$, the latter survives due to a gauge frustration mechanism. Fermions delocalize by forming bound quasiparticles with topological defects created in an otherwise dimerized electric-field background.

Topologically...
to relatively sma...
system's parame...
model of spinles...
evidence of topo...
flux is spontane...
topological orde...
symmetry-protec...
edge states and i...
these features th...
allowing topolog...
at finite chemical...
fermions and for...
for 2D gauge the...
quantum simulat...

...e usually restricted
...fine-tunning of the
...k, we investigate a
...d ladder and show
...w how a magnetic
...ility, giving rise to
...exists here with a
...lized gauge-matter
...l the robustness of
...n in spin liquids,
...lar, we show how,
...on, which bound to
...an ideal candidate
...d using cold-atom

...ular Physics,
...Physics,

Systems:

"Paradigmatic", notoriously difficult, but relevant systems

Fundamental systems of condensed matter, HEP and QFT

Novel Quantum sImulAtors (NOQIA)

Novel systems, novel physics

Diagnostics/Design

Single cite/single "particle" resolution

Entanglement/topology characterization (random unitaries)

Entanglement characterization (experiment-friendly approaches)

Topology characterization (experiment-friendly approaches)

Synthetic dimensions

Single-atom imaging of fermions in a quantum-gas microscope

Elmar Haller, James Hudson, Andrew Kelly, Dylan A. Cotta, Bruno Peaudecerf, Graham D. Bruce[†] and Stefan Kuhr[*]

Single-atom-resolved detection in optical lattices using quantum-gas microscopes[1,2] has enabled a new generation of experiments in the field of quantum simulation. Although such devices have been realized with bosonic species, a fermionic quantum-gas microscope has remained elusive. Here we demonstrate single-site- and single-atom-resolved fluorescence imaging of fermionic potassium-40 atoms in a quantum-gas microscope set-up, using electromagnetically-induced-transparency cooling[3,4]. We detected on average 1,000 fluorescence photons from a single atom within 1.5 s, while keeping it close to the vibrational ground state of the optical lattice. A quantum simulator for fermions with single-particle access will be an excellent test bed to investigate phenomena and properties of strongly correlated fermionic quantum systems, allowing direct measurement of ordered quantum phases[5-9] and out-of-equilibrium dynamics[10,11], with access to quantities ranging from spin–spin correlation functions to many-particle entanglement[12].

quantum systems[12]. It could perform quantum simulation of the Fermi–Hubbard model, which is conjectured to capture the key mechanism behind high-T_c superconductors, allowing researchers to gain insight into electronic properties that could potentially be applied in future materials engineering.

To achieve single-site-resolved detection of individual atoms on the lattice, it is desirable to maximize the fluorescence yield while at the same time maintaining a negligible particle loss rate and preventing the atoms from hopping between lattice sites. These conditions can be efficiently achieved by simultaneously laser cooling the atoms to sub-Doppler temperatures while detecting the fluorescence photons emitted during this process. However, cooling of fermionic alkaline atoms in optical lattices is challenging, as their low mass and small excited-state hyperfine splitting make it more difficult to obtain low temperatures using the standard technique of polarization-gradient cooling.

In this work, we achieved single-atom-resolved fluorescence imaging of ^{40}K using electromagnetically-induced-transparency

Single-

quantu

Elmar Haller, . Bruce[†]

and Stefan K

Single-atom-res

quantum-gas m

of experiments

such devices h

fermionic quan

Here we demon

fluorescence im

quantum-gas m

induced-transpa

1,000 fluoresce

while keeping i

the optical latti

single-particle

investigate phe

fermionic quan

of ordered qua

mics[10,11], with a

correlation func

imulation of the

capture the key

wing researchers

ld potentially be

ndividual atoms

uorescence yield

particle loss rate

een lattice sites.

ultaneously laser

hile detecting the

However, cooling

llenging, as their

ng make it more

lard technique of
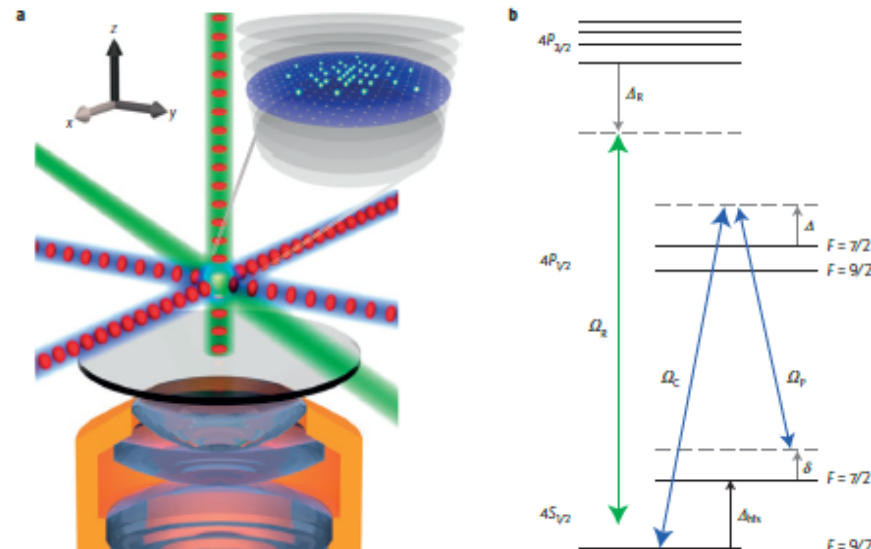
ved fluorescence

ced-transparency

Figure 1 | Experimental set-up, laser beam configuration and level scheme. a, Fermionic ^{40}K atoms in an optical lattice were observed using fluorescence detection with a high-resolution optical microscope (NA = 0.68, working distance = 12.8 mm; see ref. 2). The optical lattice (red dots) is composed of two retroreflected beams in the x- and y-axes, and a vertical beam retroreflected from the coated vacuum window. Retroreflected EIT cooling beams (blue) were overlapped with the horizontal optical lattice. Raman beams (green) were used to couple the motional states in the z-axis to the horizontal plane. Atoms were prepared in the focal plane of the microscope objective (inset). **b,** Level scheme of the relevant states of ^{40}K, with off-resonant Raman beams (green) and near-resonant (detuning Δ) EIT coupling and probe beams (Rabi frequencies Ω_C and Ω_P, blue) with relative detuning $\Delta_{hfs} + \delta$.
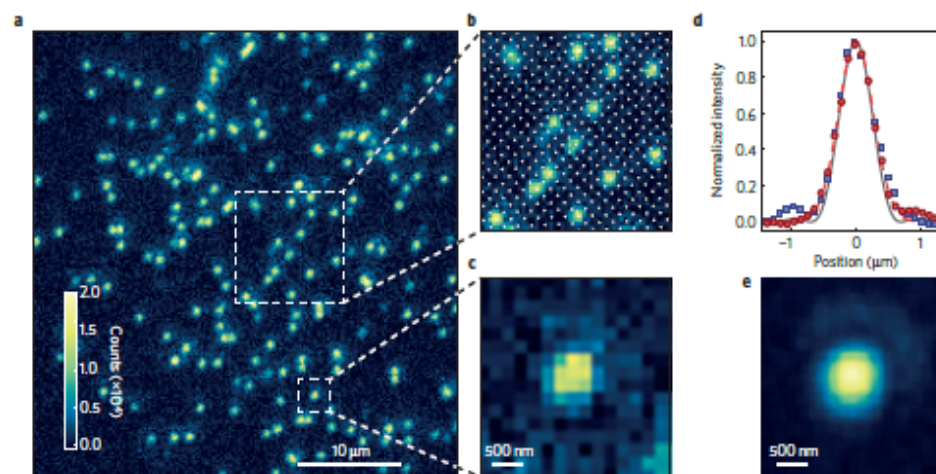

Figure 2 | Single-atom-resolved fluorescence images of fermions. a, Fluorescence image of a dilute cloud of ^{40}K atoms in the optical lattice (1.5 s exposure time with EIT cooling). **b,** 10 μm × 10 μm subsection of **a**: white dots mark the lattice sites. **c,** Magnified subsection of **a** showing an individual atom. **d,** Horizontal (red circles) and vertical (blue squares) profiles through the centre of the averaged single-atom images shown in **e**, fitted (horizontal only) with a Gaussian profile (red dashed line). The grey line shows the diffraction-limited point-spread function (PSF) of the microscope objective. **e,** Measured point-spread function using 640 single-atom images as presented in **c**, averaged using subpixel shifting[3].

Systems:

"Paradigmatic", notoriously difficult, but relevant systems

Fundamental systems of condensed matter, HEP and QFT

Novel Quantum sImulAtors (NOQIA)

Novel systems, novel physics

Diagnostics/Design

Single cite/single "particle" resolution

Entanglement/topology characterization (random unitaries)

Entanglement characterization (experiment-friendly approaches)

Topology characterization (experiment-friendly approaches)

Synthetic dimensions

Many-body Chern number from statistical correlations of randomized measurements

Ze-Pei Cian,[1,2] Hossein Dehghani,[1,2] Andreas Elben,[3,4] Benoît Vermersch,[3,4,5]

Guanyu Zhu,[6] Maissam Barkeshli,[1,7] Peter Zoller,[3,4] and Mohammad Hafezi[1,2]

[1]*Joint Quantum Institute, College Park, 20742 MD, USA*
[2]*The Institute for Research in Electronics and Applied Physics,*
University of Maryland, College Park, 20742 MD, USA
[3]*Center for Quantum Physics, University of Innsbruck, Innsbruck A-6020, Austria.*
[4]*Institute for Quantum Optics and Quantum Information of the Austrian Academy of Sciences, Innsbruck A-6020, Austria.*
[5]*Univ. Grenoble Alpes, CNRS, LPMMC, 38000 Grenoble, France.*
[6]*IBM T.J. Watson Research Center, Yorktown Heights, New York 10598, USA.*
[7]*Condensed Matter Theory Center, Department of Physics,*
University of Maryland, College Park, 20742 MD, USA
(Dated: May 29, 2020)

One of the main topological invariants that characterizes several topologically-ordered phases is the many-body Chern number (MBCN). Paradigmatic examples include several fractional quantum Hall phases, which are expected to be realized in different atomic and photonic quantum platforms in the near future. Experimental measurement and numerical computation of this invariant is conventionally based on the linear-response techniques which require having access to a family of states, as a function of an external parameter, which is not suitable for many quantum simulators. Here, we propose an ancilla-free experimental scheme for the measurement of this invariant, without requiring any knowledge of the Hamiltonian. Specifically, we use the statistical correlations of randomized measurements to infer the MBCN of a wavefunction. Remarkably, our results apply to disk-like geometries that are more amenable to current quantum simulator architectures.
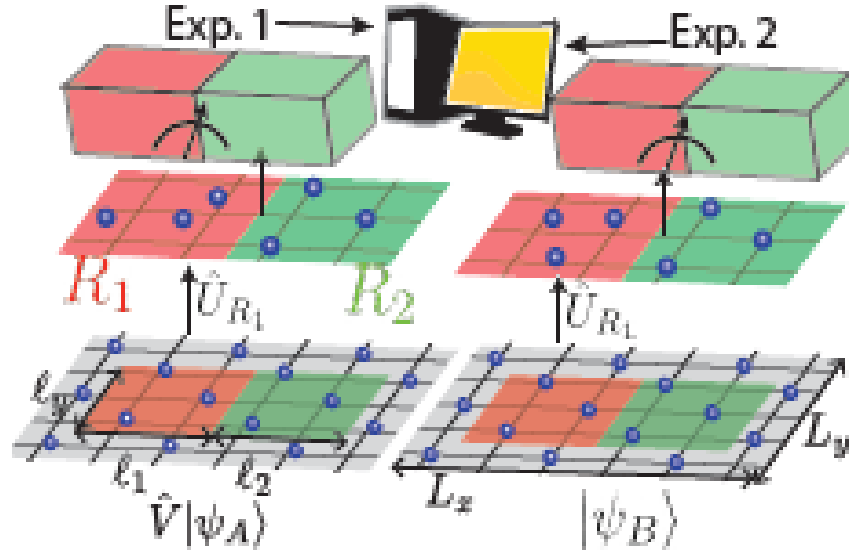
Many-body ... :d measurements

FIG. 1: The randomized measurement scheme. We define two regions R_1 (red) and R_2 (green) in the lattice with side length $\ell_1 \times \ell_y$ and $\ell_2 \times \ell_y$ respectively. We prepare two identical wave functions $|\psi_A\rangle$ and $|\psi_B\rangle$ in experiment A and B respectively. The local unitary operator $\hat{V}$ is applied in the region R_1 in the exp. 1. Subsequently, the random unitary $\hat{U}_{R_1}$ is applied in the region R_1 on both wave functions. The projective measurements on the particle occupation basis are performed on regions R_1 and R_2 in both experiments. The MBCN can be inferred from the statistical correlation between the randomized measurement results in experiment A and experiment B.

^{4}Institute for Qua

Entanglement Hamiltonian Tomography in Quantum Simulation

Christian Kokail,[1,2] Rick van Bijnen,[1,2] Andreas Elben,[1,2] Benoît Vermersch,[1,2,3] and Peter Zoller[1,2]

[1]*Center for Quantum Physics, University of Innsbruck, Innsbruck, Austria*
[2]*Institute for Quantum Optics and Quantum Information of the Austrian Academy of Sciences, Innsbruck, Austria*
[3]*Univ. Grenoble Alpes, CNRS, LPMMC, 38000 Grenoble, France*

Entanglement is the crucial ingredient of quantum many-body physics, and characterizing and quantifying entanglement in closed system dynamics of quantum simulators is an outstanding challenge in today's era of intermediate scale quantum devices. Here we discuss an efficient tomographic protocol for reconstructing reduced density matrices and entanglement spectra for spin systems. The key step is a parametrization of the reduced density matrix in terms of an entanglement Hamiltonian involving only quasi local few-body terms. This ansatz is fitted to, and can be independently verified from, a small number of randomised measurements. The ansatz is suggested by Conformal Field Theory in quench dynamics, and via the Bisognano-Wichmann theorem for ground states. Not only does the protocol provide a testbed for these theories in quantum simulators, it is also applicable outside these regimes. We show the validity and efficiency of the protocol for a long-range Ising model in 1D using numerical simulations. Furthermore, by analyzing data from 10 and 20 ion quantum simulators [Brydges *et al.*, Science, 2019], we demonstrate measurement of the evolution of the entanglement spectrum in quench dynamics.
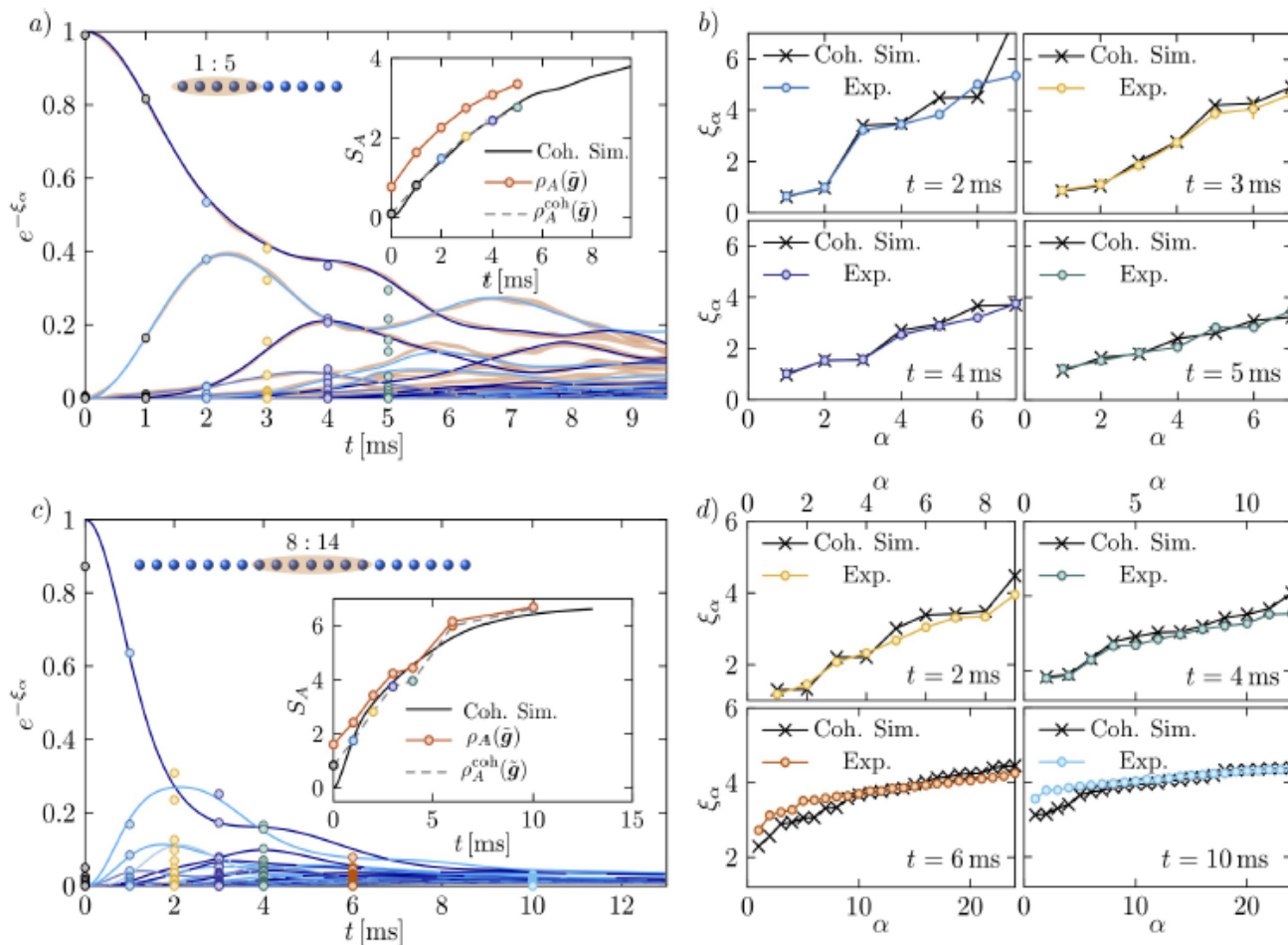
FIG. 1. *EHT in experimental quench dynamics*: Time evolution of the ES $\{\lambda_\alpha^2 \equiv e^{-\xi_\alpha}\}$ in Hamiltonian quench dynamics with a long-range transverse-field Ising model (2) ($B \gg J$) from an initial Nèel state $|\uparrow\downarrow\uparrow \ldots\rangle$ on 10 and 20-spin trapped-ion quantum simulators, for 5 and 7-spin partitions, as shown in the insets. a), c) ES as a function of time. Colored circles show the eigenvalues of $\rho_A^{coh}(\tilde{g})$ (defined in Eq. (A2) in the), obtained from EHT on experimental data with $N_M = 150$ measurements taken in $N_U = 500$ different random bases. Solid lines show theoretical simulations of the Hamiltonian quench dynamics, with different colors indicating the total magnetization of the Schmidt components. Orange colored bands in a) show the 68% confidence interval obtained by repeatedly simulating the full EHT procedure with the same settings on the entire time interval. Insets in a) and c): von Neumann entanglement entropy $S_A = -\text{Tr}(\rho_A \log_2 \rho_A)$ as a function of time. Black solid line indicates exact results from simulation of coherent Hamiltonian dynamics. Colored points show S_A extracted from EHT on experimental data, obtained from the spectrum of $\rho_A^{coh}(\tilde{g})$, while orange points show S_A obtained from the full ansatz (see Eq. (A2) in Appendix A) including imperfect initial state preparation and measurement errors. b), d) Reconstructed lowest eigenvalues $\{\xi_\alpha\}$ of the EH in EHT at later times, and comparison with ES obtained from numerical simulations of exact Hamiltonian dynamics. Error bars, calculated via Jackknife resampling, are mostly smaller than symbols.

Systems:

"Paradigmatic", notoriously difficult, but relevant systems

Fundamental systems of condensed matter, HEP and QFT

Novel Quantum sImulAtors (NOQIA)

Novel systems, novel physics

Diagnostics/Design

Single cite/single "particle" resolution

Entanglement/topology characterization (random unitaries)

Entanglement characterization (experiment-friendly approaches)

Topology characterization (experiment-friendly approaches)

Synthetic dimensions

QUANTUM NONLOCALITY

Detecting nonlocality in many-body quantum states

J. Tura,[1] R. Augusiak,[1*] A. B. Sainz,[1] T. Vértesi,[2] M. Lewenstein,[1,3] A. Acín[1,3]

Intensive studies of entanglement properties have proven essential for our understanding of quantum many-body systems. In contrast, much less is known about the role of quantum nonlocality in these systems because the available multipartite Bell inequalities involve correlations among many particles, which are difficult to access experimentally. We constructed multipartite Bell inequalities that involve only two-body correlations and show how they reveal the nonlocality in many-body systems relevant for nuclear and atomic physics. Our inequalities are violated by any number of parties and can be tested by measuring total spin components, opening the way to the experimental detection of many-body nonlocality, for instance with atomic ensembles.

$$\sum_{i=1}^{N}\left(\alpha_i\langle\mathcal{M}_0^{(i)}\rangle+\beta_i\langle\mathcal{M}_1^{(i)}\rangle\right)+\sum_{i<j}^{N}\gamma_{ij}\langle\mathcal{M}_0^{(i)}\mathcal{M}_0^{(j)}\rangle+$$

$$\sum_{i\neq j}^{N}\delta_{ij}\langle\mathcal{M}_0^{(i)}\mathcal{M}_1^{(j)}\rangle+\sum_{i<j}^{N}\varepsilon_{ij}\langle\mathcal{M}_1^{(i)}\mathcal{M}_1^{(j)}\rangle+$$

$$\beta_C\geq 0 \qquad\qquad (2)$$

Bell Correlations at Ising Quantum Critical Points

Angelo Piga,[1,*] Albert Aloy,[1] Maciej Lewenstein,[1,2] and Irénée Frérot[1,†]

[1]*ICFO-Institut de Ciencies Fotoniques, The Barcelona Institute of Science and Technology,*
Av. Carl Friedrich Gauss 3, 08860 Barcelona, Spain
[2]*ICREA-Institució Catalana de Recerca i Estudis Avançats, Lluis Companys 23, 08010 Barcelona, Spain*

When a collection of distant observers share an entangled quantum state, the statistical correlations among their measurements may violate a many-body Bell inequality, demonstrating a nonlocal behavior. Focusing on the Ising model in a transverse field with power-law ($1/r^\alpha$) ferromagnetic interactions, we show that a permutationally invariant Bell inequality based on two-body correlations is violated in the vicinity of the quantum-critical point. This observation, obtained via analytical spin-wave calculations and numerical density-matrix renormalization group computations, is traced back to the squeezing of collective-spin fluctuations generated by quantum-critical correlations. We observe a maximal violation for infinite-range interactions ($\alpha = 0$), namely, when interactions and correlations are themselves permutationally invariant.

Bell

Angelo I

[1,†]

^{1}ICFO-Institut a

chnology,

^{2}ICREA-Institució Cat

Barcelona, Spain

When a collection ... cal correlations
among their measuren ... nlocal behavior.
Focusing on the Ising ... nteractions, we
show that a permutati ... violated in the
vicinity of the quantur ... alculations and
numerical density-ma ... squeezing of
collective-spin fluctua ... ximal violation
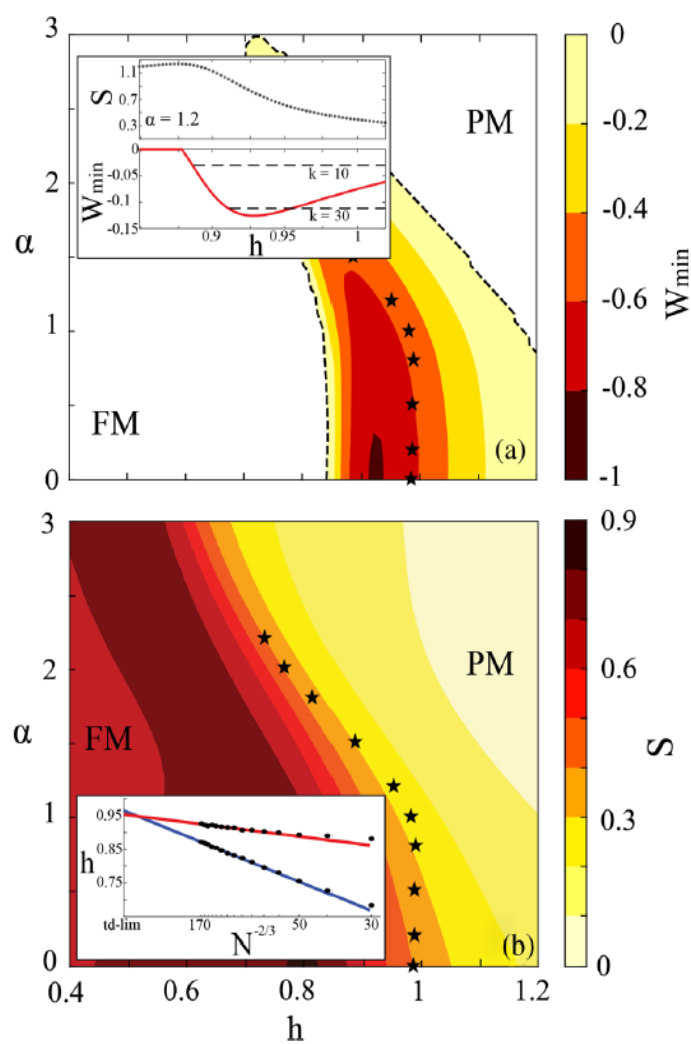for infinite-range int ... are themselves
permutationally invari

FIG. 1. (a) BI violation and (b) bipartite EE (b) for the one-dimensional long-range TFIM ($N = 40$). Stars are extrapolations for $N \to \infty$ of the maximum of EE. Inset in (a): bipartite EE and maximal violation of BI Eq. (1) for $N = 170$ and $\alpha = 1.2$. Black dashed lines: k-producibility bounds [22] (see text) for $k = 10$ and $k = 30$. Inset in (b): critical point extrapolated for $N \to \infty$. Both maximum of EE and maximal violation of the BI occur for the same transverse field. Fits of the form $h_c(N) = h_c(\infty) + aN^{-2/3}$ [26].

Systems:

"Paradigmatic", notoriously difficult, but relevant systems

Fundamental systems of condensed matter, HEP and QFT

Novel Quantum sImulAtors (NOQIA)

Novel systems, novel physics

Diagnostics/Design

Single cite/single "particle" resolution

Entanglement/topology characterization (random unitaries)

Entanglement characterization (experiment-friendly approaches)

Topology characterization (experiment-friendly approaches)

Synthetic dimensions

Simulating Twistronics without a Twist

Tymoteusz Salamon[ORCID],[1] Alessio Celi[ORCID],[2] Ravindra W. Chhajlany[ORCID],[3] Irénée Frérot[ORCID],[1,4] Maciej Lewenstein,[1,5] Leticia Tarruell[ORCID],[1] and Debraj Rakshit[ORCID][1,4]

[1]ICFO—Institut de Ciencies Fotoniques, The Barcelona Institute of Science and Technology, 08860 Castelldefels (Barcelona), Spain

[2]Departament de Física, Universitat Autònoma de Barcelona, 08193 Bellaterra, Spain

[3]Faculty of Physics, Adam Mickiewicz University, 61614 Poznan, Poland

[4]Max-Planck-Institut für Quantenoptik, D-85748 Garching, Germany

[5]Institució Catalana de Recerca i Estudis Avançats (ICREA), Passeig Lluis Companys 23, ES-08010 Barcelona, Spain

Rotational misalignment or twisting of two monolayers of graphene strongly influences its electronic properties. Structurally, twisting leads to large periodic supercell structures, which in turn can support intriguing strongly correlated behavior. Here, we propose a highly tunable scheme to synthetically emulate twisted bilayer systems with ultracold atoms trapped in an optical lattice. In our scheme, neither a physical bilayer nor twist is directly realized. Instead, two synthetic layers are produced exploiting coherently coupled internal atomic states, and a supercell structure is generated via a spatially dependent Raman coupling. To illustrate this concept, we focus on a synthetic square bilayer lattice and show that it leads to tunable quasiflatbands and Dirac cone spectra under certain magic supercell periodicities. The appearance of these features are explained using a perturbative analysis. Our proposal can be implemented using available state-of-the-art experimental techniques, and opens the route toward the controlled study of strongly correlated flatband accompanied by hybridization physics akin to magic angle bilayer graphene in cold atom quantum simulators.

Tymoteusz Salamon [ORCID]

[1]ICFO—Ins

[2]Departo
[3]I

Maciej Lewenstein,[1,5]

Technology,

a, Spain
d

(2020)

Rotational mis   ces its electronic
properties. Struct   turn can support
intriguing strongl   netically emulate
twisted bilayer sy   either a physical
bilayer nor twist   iting coherently
coupled internal   ependent Raman
coupling. To illus   w that it leads to
tunable quasiflatl   . The appearance
of these features   plemented using
available state-of   ntrolled study of
strongly correlate   ayer graphene in
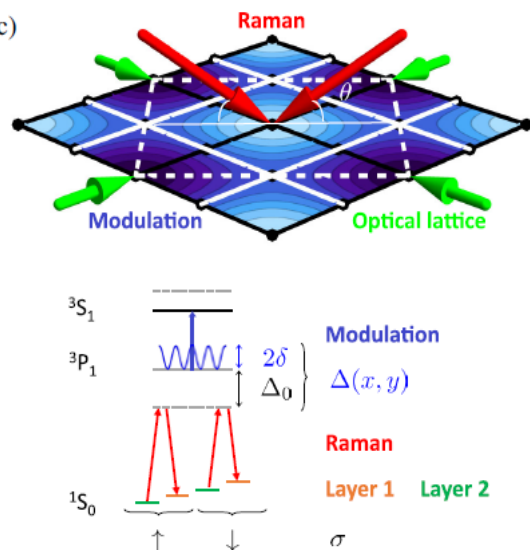cold atom quantu
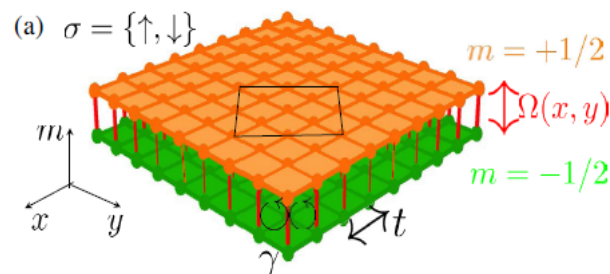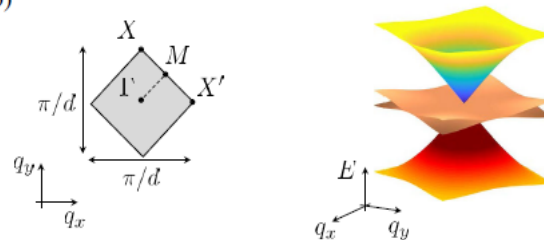
FIG. 1.   Synthetic bilayer structure with a supercell. (a) Real-
space potential of the synthetic bilayer. Each plane corresponds to
one spin state $m = \pm 1/2$ (orange, green), which experiences a
square lattice potential (tunneling t) and is connected to the other
layer by a spatially dependent and complex coupling $\Omega(x, y)$
(vertical red lines of variable width). A top view of the lattice
indicating the unit cell of the system containing 2×8 sites for
$l_x = l_y = 4d$ is shown (black line). (b) Sketch of the first

Methods (theory)

Tensor networks (DMRG, MPS, PEPS, MERA…)

Exact diagonalization

Semi-definite programming

Machine learning

Stripes, Antiferromagnetism, and the Pseudogap in the Doped Hubbard Model at Finite Temperature

Alexander Wietek,[1, *] Yuan-Yao He,[1] Steven R. White,[2] Antoine Georges,[1, 3, 4, 5] and E. Miles Stoudenmire[1]

[1] *Center for Computational Quantum Physics, Flatiron Institute, 162 Fifth Avenue, New York, NY 10010, USA*
[2] *Department of Physics and Astronomy, University of California, Irvine, CA 92697-4575 USA*
[3] *Collège de France, 11 place Marcelin Berthelot, 75005 Paris, France*
[4] *CPHT, CNRS, École Polytechnique, IP Paris, F-91128 Palaiseau, France*
[5] *DQMP, Université de Genève, 24 quai Ernest Ansermet, CH-1211 Genève, Suisse*
(Dated: September 24, 2020)

The interplay between thermal and quantum fluctuations controls the competition between phases of matter in strongly correlated electron systems. We study finite-temperature properties of the strongly coupled two-dimensional doped Hubbard model using the minimally-entangled typical thermal states (METTS) method on width 4 cylinders. We discover that a novel phase characterized by commensurate short-range antiferromagnetic correlations and no charge ordering occurs at temperatures above the half-filled stripe phase extending to zero temperature. The transition from the antiferromagnetic phase to the stripe phase takes place at temperature $T/t \approx 0.05$ and is accompanied by a step-like feature of the specific heat. We find the single-particle gap to be smallest close to the nodal point at $k = (\pi/2, \pi/2)$ and detect a maximum in the magnetic susceptibility. These features bear a strong resemblance to the pseudogap phase of high-temperature cuprate superconductors. The simulations are verified using a variety of different unbiased numerical methods in the three limiting cases of zero temperature, small lattice sizes, and half-filling.

Shi-Ju Ran · Emanuele Tirrito
Cheng Peng · Xi Chen
Luca Tagliacozzo · Gang Su
Maciej Lewenstein

Tensor Network Contractions

Methods and Applications to Quantum Many-Body Systems

Methods (theory)

Tensor networks (DMRG, MPS, PEPS, MERA…)

Exact diagonalization

Semi-definite programming

Machine learning

Polynomially Filtered Exact Diagonalization Approach to Many-Body Localization

Piotr Sierant[1,2,*] Maciej Lewenstein[2,3,†] and Jakub Zakrzewski[1,4,‡]

[1]*Institute of Theoretical Physics, Jagiellonian University in Krakow, Łojasiewicza 11, 30-348 Kraków, Poland*
[2]*ICFO - Institut de Ciencies Fotoniques, The Barcelona Institute of Science and Technology,
Av. Carl Friedrich Gauss 3, 08860 Castelldefels (Barcelona), Spain*
[3]*ICREA, Pg. Lluís Companys 23, 08010 Barcelona, Spain*
[4]*Mark Kac Complex Systems Research Center, Jagiellonian University in Krakow,
Łojasiewicza 11, 30-348 Kraków, Poland*

Polynomially filtered exact diagonalization method (POLFED) for large sparse matrices is introduced. The algorithm finds an optimal basis of a subspace spanned by eigenvectors with eigenvalues close to a specified energy target by a spectral transformation using a high order polynomial of the matrix. The memory requirements scale better with system size than in the state-of-the-art shift-invert approach. The potential of POLFED is demonstrated examining many-body localization transition in 1D interacting quantum spin-1/2 chains. We investigate the disorder strength and system size scaling of Thouless time. System size dependence of bipartite entanglement entropy and of the gap ratio highlights the importance of finite-size effects. We discuss possible scenarios regarding the many-body localization transition obtaining estimates for the critical disorder strength.
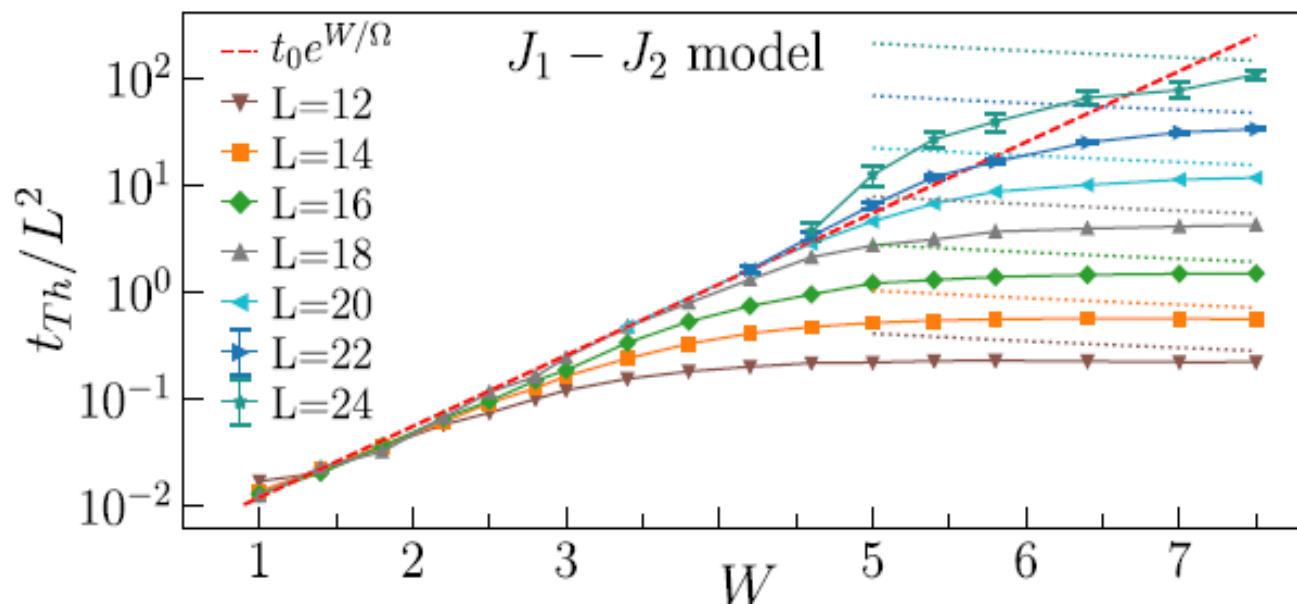
FIG. 2. Thouless time t_{Th} for system size L and disorder strength W for J_1-J_2 model. The dotted lines denote Heisenberg time t_H; the dashed line denotes a scaling $t_{Th} \propto L^2 e^{W/\Omega}$ broken by the $L = 22, 24$ data.

Methods (theory)

Tensor networks (DMRG, MPS, PEPS, MERA…)

Exact diagonalization

Semi-definite programming

Machine learning

Identifying quantum phase transitions using artificial neural networks on experimental data

Benno S. Rem[1,2], Niklas Käming[1], Matthias Tarnowski[1,2], Luca Asteria[1], Nick Fläschner[1],
Christoph Becker[1,3], Klaus Sengstock[1,2,3]* and Christof Weitenberg[1,2]

Machine-learning techniques such as artificial neural networks are currently revolutionizing many technological areas and have also proven successful in quantum physics applications[1-4]. Here, we employ an artificial neural network and deep-learning techniques to identify quantum phase transitions from single-shot experimental momentum-space density images of ultracold quantum gases and obtain results that were not feasible with conventional methods. We map out the complete two-dimensional topological phase diagram of the Haldane model[5-7] and provide an improved characterization of the superfluid-to-Mott-insulator transition in an inhomogeneous Bose–Hubbard system[8-10]. Our work points the way to unravel complex phase diagrams of general experimental systems, where the Hamiltonian and the order parameters might not be known.

the Bose–Hubbard model, both realized employing cold atoms in optical lattices. We show that we can perform tasks that were not possible with conventional techniques, such as the determination of non-local topological order from a single-shot image—a problem for which there is no physical model—and a localization of the superfluid-to-Mott-insulator transition, superior to the usual determination via interference contrast. Our examples show that machine learning can help in the identification of observables that were not previously obvious.

In a first set of experiments, we consider the Haldane model on the honeycomb lattice[5], a paradigmatic model for topological bands without a net magnetic flux possessing possible Chern numbers $C = -1, 0, 1$ (inset in Fig. 2b). The topological phase diagram is spanned by the Peierls phase Φ and the sublattice energy offset Δ_{AB}, which quantify the breaking of time-reversal symmetry

two Chern numbers in a small transition region with a full width of 100–200 Hz, which is due to the inhomogeneity of the system.

We use the same trained network to map out the entire two-dimensional phase diagram using just a few images per parameter set. In Fig. 2c we plot the expectation value of the Chern number $C = \sum_{C=-1}^{1} C \times P_C$ as a function of the shaking frequency and shaking phase. The network identifies the two lobes with Chern numbers −1 and +1, which are characteristic for the Haldane model, in quantitative agreement with a numerical calculation of the Floquet system (see Methods). The identification from single snapshots allows mapping out the full two-dimensional Haldane phase diagram.

Fig. 2 | Mapping out a topological phase diagram using a neural network. a, Examples of single experimental images of ultracold fermionic atoms released from the driven optical lattice. The shaking phase is $\phi = -90°$ and the shaking frequencies are $\omega/2\pi = 5.0$ kHz ($C=0$), $\omega/2\pi = 6.4$ kHz ($C=1$) and $\omega/2\pi = 7.8$ kHz ($C=0$), respectively. The images are 151×151 pixels in size centred around zero momentum and include the full first Brillouin zone (white hexagon). **b**, Probability for the different Chern number classes as identified by the trained neural network. The network was trained for Floquet frequencies far away from the phase transitions (grey, thin short lines in **c**). The probability is averaged over the results for 47 individual images and the error bars denote Clopper–Pearson 68% confidence intervals using the Wald method. We identify the positions of the phase transitions at 6.124(3) kHz and 6.869(3) kHz by fitting an error function to the data and extracting the point of 50% probability. The dashed lines show the transitions as expected from an ab initio numerical calculation. The inset illustrates the tight-binding scheme of the Haldane model with the staggered fluxes through the subplaquettes. **c**, The Haldane-like phase diagram of the Floquet system obtained from 10,436 evaluated test images (3–7 images per parameter) using a neural network trained at the parameters indicated by the grey lines (in total 15,963 images for training and 3,992 images for validation of the network). The training regions cover only 3% of the phase diagram. The solid lines indicate the predicted phase transitions from our ab initio numerical calculation. **d**, The circles show the positions of the phase transitions for circular shaking ($\phi = -90°$) at varying lattice depths V identified by a network trained with the data at $V = 7.4\,E_r$ (see Methods). The error bars denote the width of the error function fitted to the network output as in **b**. The lines show the predicted phase transitions from our ab initio numerical calculation with the red regions indicating the systematic uncertainty calculated for an error of 0.2° on the polarization of the lattice beams. Source data for **b–d** are provided in Supplementary Data 1–3.
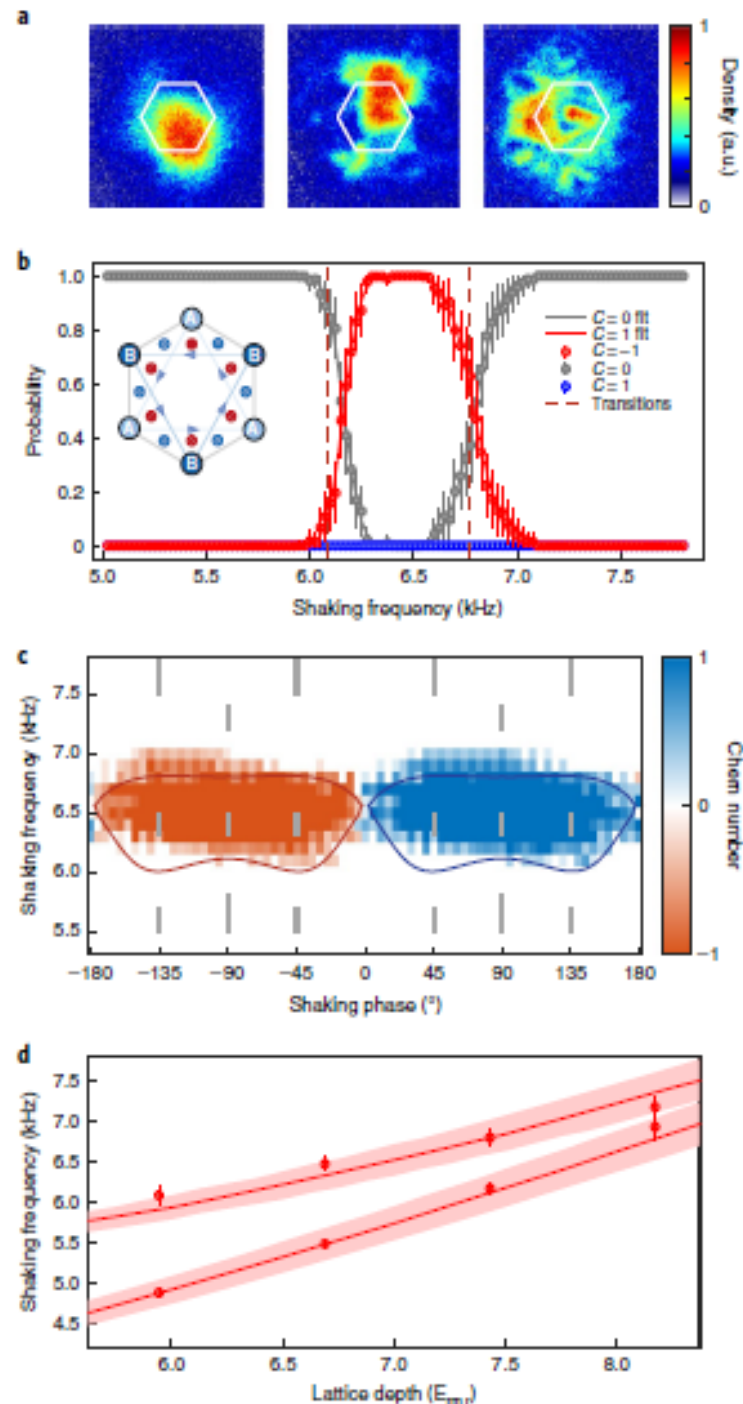
Unsupervised Phase Discovery with Deep Anomaly Detection

Korbinian Kottmann[1,*] Patrick Huembeli,[1] Maciej Lewenstein,[1,2] and Antonio Acín[1,2]

[1]*ICFO—Institut de Ciencies Fotoniques, The Barcelona Institute of Science and Technology,*
Av. Carl Friedrich Gauss 3, 08860 Castelldefels (Barcelona), Spain
[2]*ICREA, Pg. Llus Companys 23, 08010 Barcelona, Spain*

We demonstrate how to explore phase diagrams with automated and unsupervised machine learning to find regions of interest for possible new phases. In contrast to supervised learning, where data is classified using predetermined labels, we here perform anomaly detection, where the task is to differentiate a normal dataset, composed of one or several classes, from anomalous data. As a paradigmatic example, we explore the phase diagram of the extended Bose Hubbard model in one dimension at exact integer filling and employ deep neural networks to determine the entire phase diagram in a completely unsupervised and automated fashion. As input data for learning, we first use the entanglement spectra and central tensors derived from tensor-networks algorithms for ground-state computation and later we extend our method and use experimentally accessible data such as low-order correlation functions as inputs. Our method allows us to reveal a phase-separated region between supersolid and superfluid parts with unexpected properties, which appears in the system in addition to the standard superfluid, Mott insulator, Haldane-insulating, and density wave phases.

Unsupervised Phase Discovery with Deep Anomaly Detection

Hamiltonian We test our method on the extended Bose-Hubbard Model

$$H = -t \sum_i \left(b_i^\dagger b_{i+1} + b_{i+1}^\dagger b_i \right)$$

$$+ \frac{U}{2} \sum_i n_i(n_i - 1) + V \sum_i n_i n_{i+1}, \quad (3)$$

to reveal a phase-separated region between supersolid and superfluid parts with unexpected properties, which appears in the system in addition to the standard superfluid, Mott insulator, Haldane-insulating, and density wave phases.
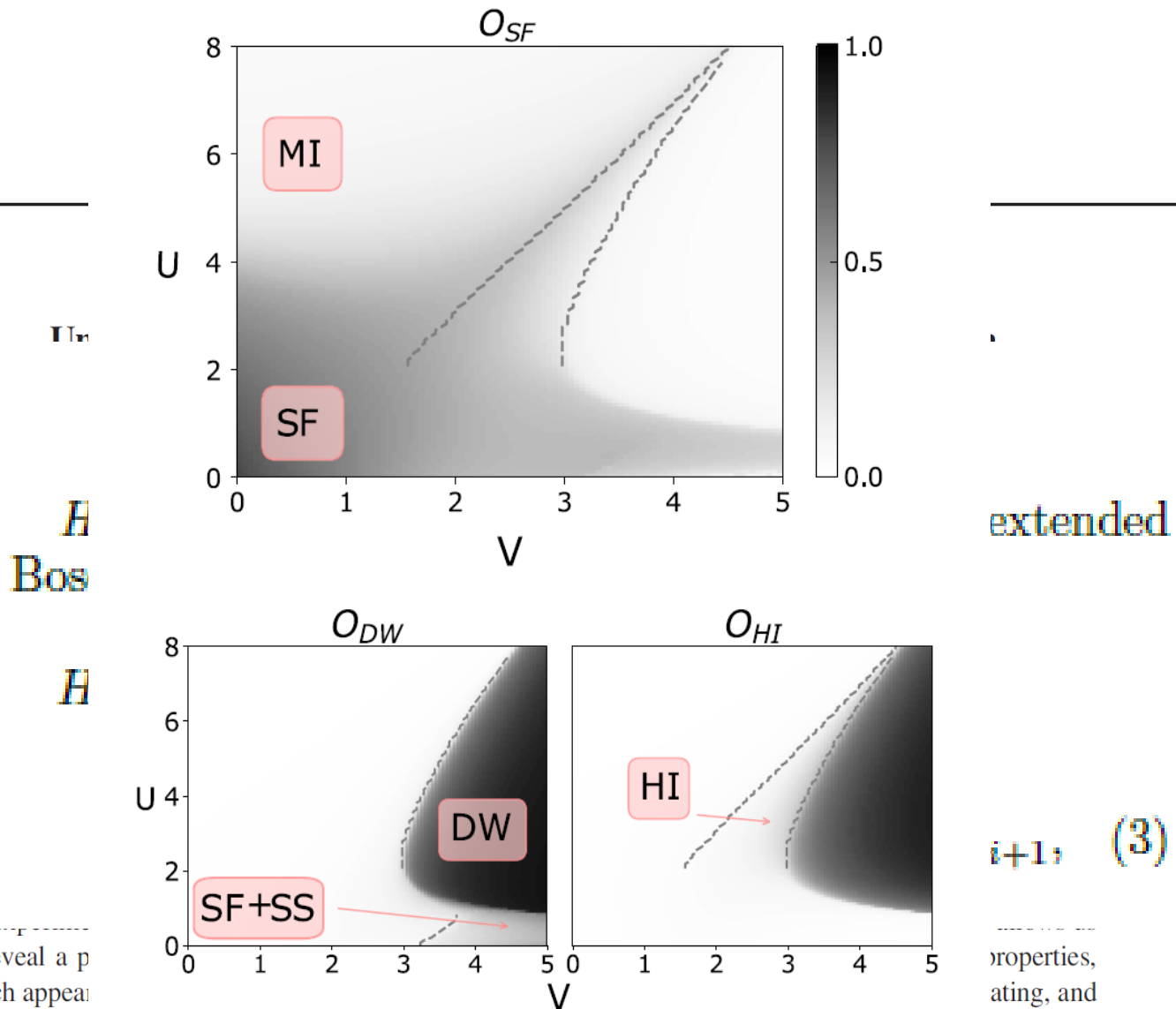
FIG. 2. Extended BH phase diagram with five distinct phases obtained by the correlators Eqs. (3)–(5). The dashed lines indicate the transition points observed from diverging correlation lengths between MI-HI-DW and nonzero $\mathcal{S}$ in Eq. (6) between SF and SF + SS.

extended

H

Bos

H

$i+1;$ (3)

Un

to reveal a p
which appea
density wave

properties,
ating, and

Conclusions?

Enjoy physics and beyond!!!